Electronic, magnetic, and structural properties of V_2CoAl: experimental and computational study

Parashu Kharel,[1] Cole Brown,[1] Brandon Schmidt,[2] Caden Sadler,[2] Salimatou Diallo,[2] Mohd Anas,[1] Paul M. Shand,[2] Pavel V. Lukashev[2,#]

[1]*Department of Chemistry, Biochemistry and Physics, South Dakota State University, Brookings, SD 57007, USA*

[2]*Department of Physics, University of Northern Iowa, Cedar Falls, IA 50614, USA*

Corresponding author: pavel.lukashev@uni.edu

Abstract

Here, we present results of combined experimental and computations study of V_2CoAl, a Heusler alloy that exhibits nearly perfect spin-polarization. Our calculations indicate that this material maintains a high degree of spin-polarization (over 90%) in the wide range of lattice parameters, except at the largest considered unit cell volume. The magnetic alignment of V_2CoAl is ferrimagnetic, due to the antialignment of the magnetic moments of vanadium atoms in their two sublattices. The calculated total magnetic moment per formula unit is nearly integer at the optimal lattice parameter and at the smaller volumes of the unit cell, but it deviated from the integer values as the unit cell expands. This is consistent with the calculated variation in the degree of spin polarization with lattice constant. The expected ferrimagnetic behavior has been observed in the arc-melted V_2CoAl sample, with a Curie temperature of about 80 K. However, the saturation magnetization is significantly smaller than the theoretical prediction of approximately $2\mu_B/f.u.$, most likely due to the observed B2-type atomic disorder. The samples exhibit metallic electron transport across the measurement range of 2 K to 300 K.

I. Introduction

The field of spin-based electronics (spintronics) is one of the most actively researched branches of materials science. One type of material that has attracted particular attention for spintronic applications is a half-metal. These materials are electric conductors for one of the spins, and insulators / semiconductors for the other spin. Thus, by definition, they exhibit 100% spin-polarization, where the latter is defined as $P = \frac{N_\uparrow(\epsilon_F) - N_\downarrow(\epsilon_F)}{N_\uparrow(\epsilon_F) + N_\downarrow(\epsilon_F)}$, with $N_{\uparrow,\downarrow}(\epsilon_F)$ being the spin-dependent density of states (DOS) at the Fermi level, ϵ_F.[1] Half-metallic compounds were predicted in 1983 in a seminal work by de Groot et al.[2] Since then, many systems, including certain oxides and manganites,[3] double perovskites,[4] chalcogenides,[5] and pyrites,[6] have been suggested to

exhibit half-metallic electronic structure. Heusler alloys have attracted particular attention, largely due to their high Curie temperature, often much higher than room temperature.[7,8,9,10,11,12,13] While direct experimental confirmation of half-metallicity is more challenging than computational predictions, there were quite a few experimental reports of half-metallic Heusler alloys.[14,15,16,17] In addition, some physical mechanisms, such as atomic disorder and surface states in thin-film geometry, may have a detrimental impact on the degree of spin-polarization of potentially half-metallic compounds.[18,19,20,21,22,23,24,25,26,27,28] Despite these challenges, half-metals are still considered among the most promising candidates for practical applications in spintronics.[29,30]

In this paper, we study electronic, magnetic, and structural properties of V_2CoAl, a Heusler compound that exhibits nearly perfect half-metallic properties in a wide range of lattice parameters. Our calculations indicate that except for the largest considered unit cell volumes (which may not be realistically achievable in practice), this alloy exhibits very high degree of spin-polarization values (over 90%). The calculated magnetization values (nearly integer in a wide range of considered lattice parameters) support the nearly half-metallic nature of this material. The magnetic alignment of V_2CoAl is ferrimagnetic, due to the magnetic moments of vanadium atoms from two different sublattices being anti-aligned. The observed ferrimagnetic behavior in the arc-melted V_2CoAl is consistent with the theoretical prediction. This study represents the first experimental report on this material to date.

The rest of the paper is organized as follows. In the next section, we present computational and experimental techniques and methods employed in this work. In Section 3, we present our main results. The concluding remarks are presented in Section 4, which is followed by acknowledgments to funding sources and computational facilities. The references to the relevant literature are presented at the end of the paper.

II. Methods

II. a) Computational methods

The computational techniques used in this work are based on density functional theory as implemented in the Vienna *ab initio* simulation package (VASP).[31] More specifically, we employed the projector augmented-wave method (PAW)[32] and generalized-gradient approximation (GGA) method proposed by Perdew, Burke, and Ernzerhof.[33] The integration method by Methfessel and Paxton was used, with a 5×10^{-2} eV width of smearing.[34] The

electronic and magnetic structure calculations are performed with a convergence criterion of 10^{-3} meV and a *k*-mesh of 8×8×8. Hubbard U correction is not implemented in this work because the considered system is metallic. In metals, the correlation effects are less important than e.g. in magnetic insulators and are usually adequetly described within regular GGA.[35] The MedeA® software environment[36] is used for calculating and plotting band structures. The reported calculations were performed using the Advanced Cyberinfrastructure Coordination Ecosystem: Services & Support (ACCESS) (formerly known as Extreme Science and Engineering Discovery Environment (XSEDE)) resources located at the Pittsburgh Supercomputing Center (PSC),[37] the resources of the Center for Functional Nanomaterials (CFN) at Brookhaven National Laboratory (BNL), as well as the high-performance computing cluster located at the University of Northern Iowa (UNI).

II. b) Experimental methods

The bulk samples of the V_2CoAl Heusler alloy were synthesized using arc melting followed by annealing. Initially, an ingot of V_2CoAl was produced by melting pieces of V, Co, and Al, made from commercially available metal pellets with a minimum purity of 99.95%, to achieve the desired stoichiometry. The melting process was conducted inside an arc furnace under a continuous flow of argon gas. Afterward, the arc-melted ingot was sealed in a quartz tube under partial argon pressure and annealed at 700°C for one week.

The crystal structure was investigated through X-ray diffraction (XRD) analysis of a powder sample, prepared by grinding the annealed ingot with a mortar and pestle. XRD patterns were recorded at room temperature using a Rigaku Miniflex600 diffractometer. Rietveld refinement of the powder XRD data was performed with the FullProf suite.[38] Magnetic measurements were carried out using magnetometers on the Quantum Design VersaLab and Dynacool PPMS platforms. Electrical transport measurements were performed using the aforementioned PPMS system.

III. Results

III. a) Computational results

Figure 1 (a) shows calculated total energy (black line and circles) and magnetic moment (blue line and squares) of V_2CoAl as a function of lattice constant. Our calculations indicate that

V_2CoAl crystallizes in the inverted cubic Heusler structure, with the equilibrium lattice parameter of $a = 5.901$ Å. See e.g. Ref. 13 for more detailed discussion of various crystal structures of Heusler compounds. As seen from Fig. 1 (b), the magnetic alignment of V_2CoAl is ferrimagnetic, due to the magnetic moments of two vanadium sub-lattices being anti-aligned. In particular, in the inverted cubic structure (which corresponds to the lowest energy), the Wyckoff positions of V_2CoAl are as follows: V_1 (0,0,0), V_2 (1/4,1/4,1/4), Co(1/2,1/2,1/2), Al(3/4,3/4,3/4). Here, by V_1 and V_2 we indicate two sub-lattices of vanadium atoms. This notation is consistent with the one used in Fig. 1 (b).

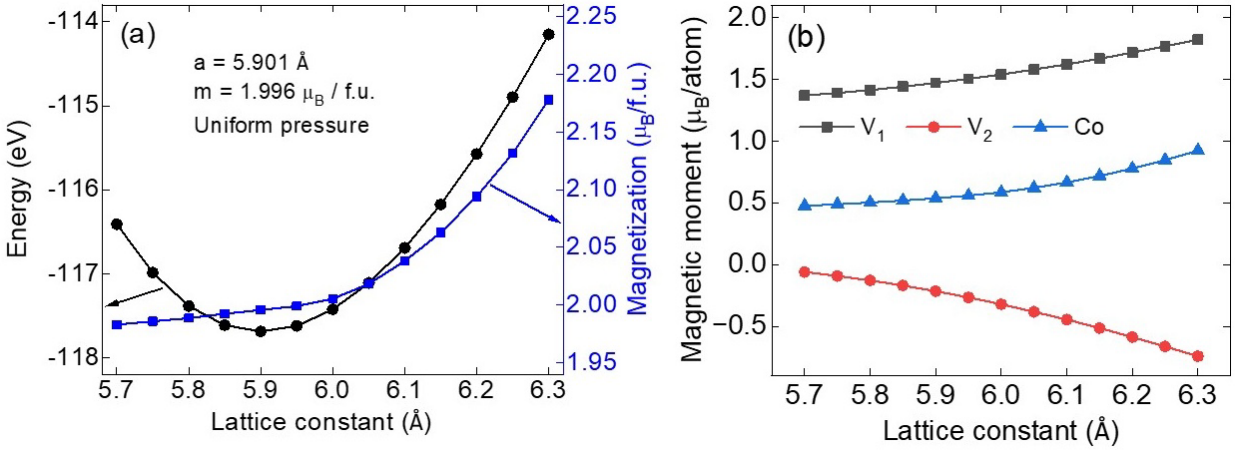

Figure 1: (a) Calculated total energy (black line and circles) and magnetic moment (blue line and squares) of V_2CoAl as a function of lattice constant. (b) Element resolved magnetitic moments of V_2CoAl as a function of lattice constant. (b). The element resolved magnetic moments are colored / labeled as indicated in the figure, i.e. V_1 – black line and squares, V_2 – red line and circles, Co – blue line and triangles.

In addition, as shown in Fig. 1 (a), the magnetization of V_2CoAl exhibits a nearly integer value at the equilibrium lattice parameter and at the compression of the volume of the unit cell. The calculated magnetization deviates from the integer value at the larger lattice parameters, thus indicating that this material may exhibit half-metallic behavior at the optimal lattice parameter and under compression, but maybe not under expansion of the unit cell..[39]

Figure 2 shows calculated total and element resolved density of states (a) and electronic band structure (b) of V_2CoAl at the equilibrium lattice constant, as well as the calculated total density of states of this compound for different lattice constants (indicated in the figure) calculated at uniform pressure (c). As seen from Fig. 2 (a), V_2CoAl exhibits nearly 100% spin-polarized electronic structure, due to the nearly gapless nature of the majority-spin states at the Fermi level. At the same time, the minority-spin states exhibit conducting behavior. This conclusion is

confirmed by analyzing the band structure of this compound shown in Fig. 2 (b). In particular, the spin-down bands (blue lines) exhibit conducting behavior, despite a large energy gap of the valence bands ~0.3 eV below Fermi level. At the same time, the majority-spin bands demonstrate a nearly gapless nature at the Γ point. As shown in Fig. 2 (c), this behavior of the energy bands / states of V_2CoAl is not very sensitive to external pressure, except for the largest considered lattice parameter of 6.100 Å, where the spin-polarization is significantly reduced (down to ~75% by absolute value) due to the shift of the Fermi level towards the majority-spin conduction states. Thus, this material behaves as a nearly perfect half-metal, except at the largest considered unit cell volumes, which may not be attainable in practice.

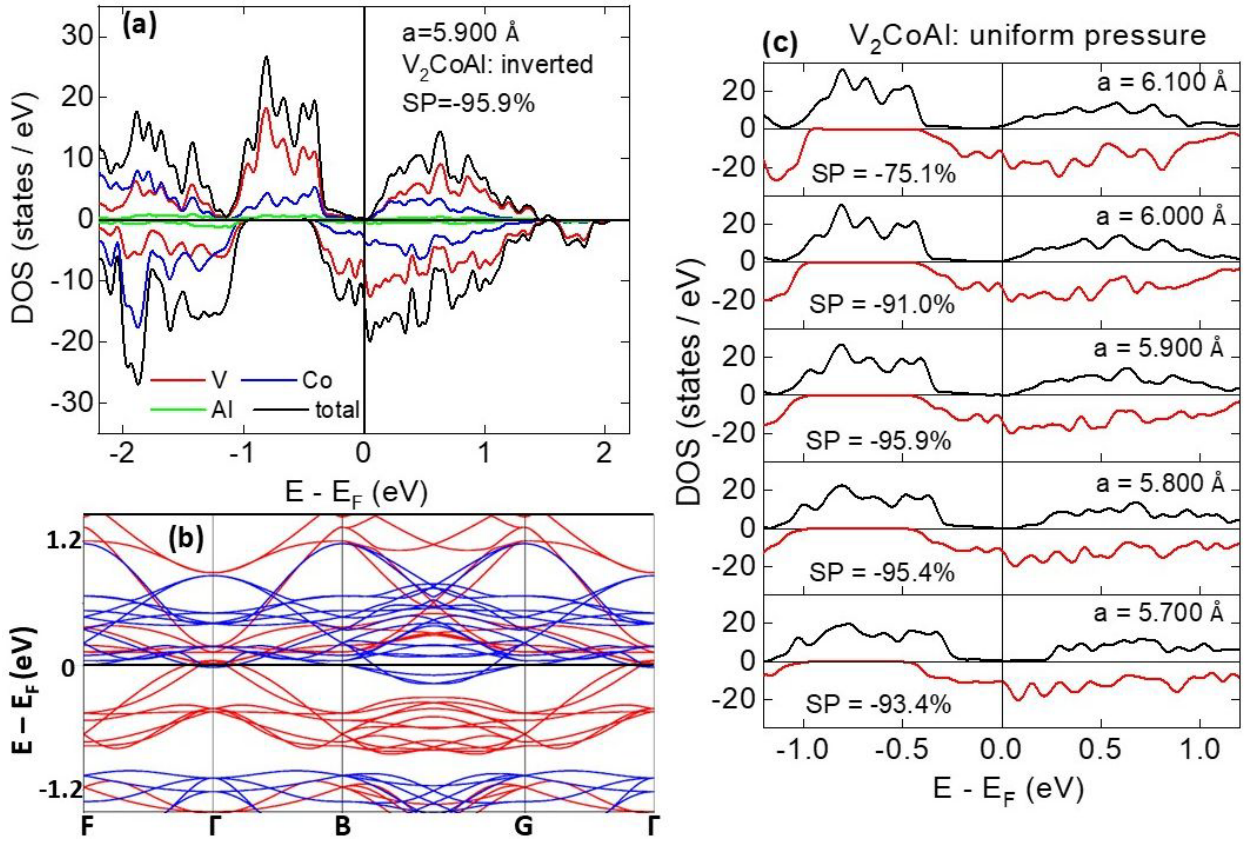

Figure 2: (a) Calculated total and element resolved density of states of V_2CoAl at the equilibrium lattice constant. The vertical line corresponds to the Fermi level. Positive / negative DOS represents spin-up / spin-down states, correspondingly. Element resolved density of states are colored as indicated in the figure: red – V, blue – Co, green – Al, black – total. (b) Calculated band structures of V_2CoAl at the equilibrium lattice constant (the symmetry points of the Brillouin zone are generated by the MedeA software package). The horizontal line in the middle of the plot corresponds to the Fermi level. Red / blue lines represents spin-up / spin-down bands, correspondingly. (c) Calculated total density of states of V_2CoAl for different lattice constants (indicated in the figure) calculated at hydrostatic pressure. The vertical line corresponds to the Fermi level. Positive (black line) / negative (red line) DOS represents spin-up / spin-down states, correspondingly.

III. b) Experimental results

Figure 3(a) shows the powder X-ray diffraction (XRD) pattern of the annealed V_2CoAl sample, recorded at room temperature. The XRD pattern is indexed with an inverted cubic Heusler structure, as predicted by theoretical calculations. The atomic site occupancy of the inverted cubic structure is illustrated in Figure 3(b). As shown, all diffraction peaks are marked with their corresponding plane indices, and no peaks from elemental impurities or alloy phases are detected. However, the (111) peak is absent, and the (200) peak is slightly weaker, suggesting that the sample exhibits B2-type disorder. It is also noted that the calculated intensities of these two peaks are much weaker compared to the other fundamental peaks.

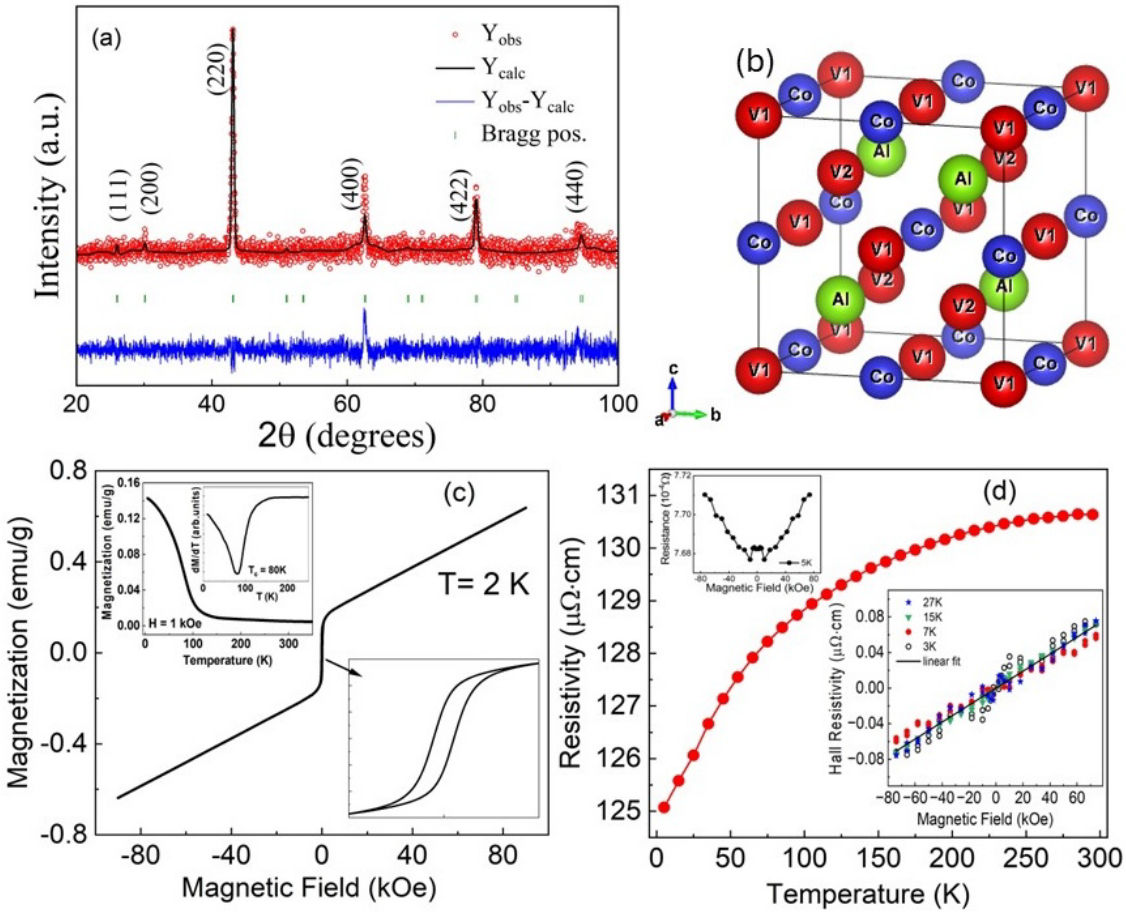

Figure 3: (a) Room-temperature x-ray diffraction pattern of the annealed V_2CoAl sample with the Rietveld refined curve. (b) Crystal structure of V_2CoAl in the inverse cubic Heusler structure. (c) Isothermal magnetization curve, M(H), of V_2CoAl measured at 2 K. The inset on the left shows the thermomagnetic curve, M(T), with the estimated Curie temperature of 80 K. The inset on the right shows an expanded M(H) curve near H = 0. (d) Temperature dependence of resistivity. The inset on the left shows the resistance as a function of magnetic field at 5 K, and the inset on the right shows Hall resistivity as a function of magnetic field at different temperatures.

The pattern simulated through Rietveld refinement of the XRD data is shown in Fig. 1(a) as a solid black line. The lattice parameter obtained from the Rietveld analysis is a = 5.934Å, which is in good agreement with the theoretically estimated equilibrium lattice constant of a = 5.901 Å. A minor mismatch in the (400) peak intensity between experimental and calculated pattern can be attributed to texturing effects. The Rietveld refinement was performed using the same atomic positions and space group (*F-43m*) employed for the inverted cubic structure, as discussed in Section III(a).

The temperature dependence of magnetization, M(T), of V_2CoAl, measured under an external magnetic field of 1 kOe, is shown in the left inset of Fig. 3(c), while the isothermal magnetization curve, M(H), recorded at 2 K, is displayed as the main figure. The expanded M(H) curve near H = 0 is also shown in the right inset.

As depicted, the thermomagnetic curve resembles that of a ferro- or ferrimagnetic material, with a Curie temperature of 80 K. However, the M(H) curve at 2 K does not reach saturation even at 90 kOe, indicating ferrimagnetic ordering in the sample, consistent with the theoretically predicted magnetic order. The sample also exhibits a small coercivity of 110 Oe at 2 K. However, the high-field (90 kOe) magnetization of 0.64 emu/g (0.02 $\mu_B/f.u.$) at 2 K is significantly lower than the theoretically expected value of nearly 2 $\mu_B/f.u.$ Given the B2-type disorder in the sample, this discrepancy can be attributed to the observed disorder, though the large magnitude of the difference is somewhat unusual. The B2 disorder has apparently pushed the system closer to antiferromagnetism, with a reduction in the overall moment and significant high-field susceptibility. We tested this hypothesis by performing additional calculations for a disordered cell. In particular, to mimic the B2-type disorder, we swapped a single Co atom with a single Al atom in a 16-atom supercell of V_2CoAl at the optimal lattice constant. This resulted in a strong reduction of magnetization to ~ 0.98 $\mu_B/f.u.$ The magnetic alignment is still ferrimagnetic, but the absolute values of the magnetic moments are reduced. In addition, the magnetic moment of the swapped Co atom is now antialignedwith the rest of the magnetic moments of Co sublattice. We also swapped two Co atoms with two Al atoms to analyze the effect of a stronger B2-type disorder. This resulted in essentially zero magnetization of the cell, as the system converged to a non-magnetic state (all atomic magnetic moments are zero). Thus, our calculations confirm that B2-type disorder in V_2CoAl may lead to a strong reduction of a magnetization, and even to a non-magnetic state.

Figure 3(d) shows the resistivity of the sample, $\rho(T)$, measured as a function of temperature. As the temperature increases above 5 K, the resistivity rises almost linearly from 125 $\mu\Omega cm$ up to 75 K, after which the slope begins to decrease, deviating from linearity reaching 131 $\mu\Omega cm$ at 300 K. Near room temperature, the resistivity approaches saturation. Note that the softening of the resistance rise occurs near the Curie temperature. This is consistent with the effects of electron-magnon scattering in the ferromagnetic state. In addition, the residual resistance ratio, defined as ρ_{300K}/ρ_{2K} is about 1.05. This type of $\rho(T)$ behavior is characteristic of metals and metallic alloys with structural disorder, where different atoms are distributed randomly in the crystal lattice.[40,41] However, the low-temperature tail, often attributed to impurities and defects, is absent in this curve. Additionally, a small positive magnetoresistance is observed in the temperature range between 2K and 300 K. A resistance versus magnetic field curve measured at 5 K is shown in the left inset of Fig. 3(d). Initially, the magnetoresistance decreases with increasing magnetic field from 0 kOe, but it begins to increase once the field reaches the coercive point. This behavior is typical of ferromagnetic or ferrimagnetic materials and is attributed mainly to two factors: the reduction in electron scattering due to decreased spin disorder and the reduction in domain wall scattering as the magnetic domains realign and consolidate with increasing magnetic field. Beyond the coercive field, the material approaches magnetic saturation, and magnon scattering is suppressed at higher fields. This should lead to a decrease in magnetoresistance.[42] The observed weak positive magnetoresistance is likely due to a comparatively sparse population of magnons at low temperatures and the attendant dominance of the small positive magnetoresistance associated with the Lorentz force. As shown in the right inset of fig. 1(d), the Hall resistivities, measured at different temperatures as a function of magnetic field, are nearly linear, indicating a dominant ordinary Hall effect. A linear fit to the Hall resistivity, assuming only the ordinary Hall effect, yields a hole-like carrier density of $6.5 \times 10^{22}\ cm^{-3}$.

IV. Conclusions

In this work, we presented a combined computational and experimental study of V_2CoAl, a Heusler compound that exhibits nearly half-metallic electronic structure in a wide range of considered lattice parameters. In particular, our calculations indicate that this material behaves as a conductor for minority-spin states, while the majority-spin states exhibit nearly gapless behavior at the Fermi level. The reported character of the energy bands / states is not very sensitive to

external pressure, except at the largest considered lattice constant. The magnetic alignment of V_2CoAl is ferrimagnetic, due to the antialignment of the magnetic moments of vanadium atoms in their two sublattices. The V_2CoAl samples prepared using arc-melting and annealing have been found to crystalize in the inverse cubic Heusler structure and show ferrimagnetic order consistent with the theoretical prediction. However, the saturation magnetization is significantly smaller than the theoretical prediction of approximately $2\mu_B/f.u.$, most likely due to the observed B2-type atomic disorder. The samples exhibit metallic electron transport across the measurement range of 2 K to 300 K with a hole-like carrier density of $6.5 \times 10^{22}\ cm^{-3}$.

Acknowledgments

This research is supported by the *National Science Foundation* (NSF) under Grant Numbers 2003828 and 2003856 via DMR and EPSCoR. This work used the Advanced Cyberinfrastructure Coordination Ecosystem: Services & Support (ACCESS) (formerly known as Extreme Science and Engineering Discovery Environment (XSEDE)), which is supported by National Science Foundation grant number ACI-1548562. This work used the XSEDE Regular Memory (Bridges 2) and Storage (Bridges Ocean) at the Pittsburgh Supercomputing Center (PSC) through allocation TG-DMR180059, and the resources of the Center for Functional Nanomaterials, which is a U.S. DOE Office of Science Facility, and the Scientific Data and Computing Center, a component of the Computational Science Initiative, at Brookhaven National Laboratory (BNL) under Contract No. DE-SC0012704. Mohd Anas is supported by U.S. Department of Energy (DOE) Established Program to Stimulate Competitive Research (EPSCoR) grant no. DE-SC0024284.

Data Availability

The data that support the findings of this study are available from the corresponding author upon reasonable request.

References

1 J. Velev, P. Dowben, E. Tsymbal, S. Jenkins, and A. Caruso, Surf. Sci. Rep. **63**, 400 (2008).
2 R. de Groot, F. Mueller, P. van Engen, and K. Buschow, Phys. Rev. Lett. **50**, 2024 (1983).
3 R. Soulen Jr, J. Byers, M. Osofsky, B. Nadgorny, T. Ambrose, S. Cheng, P. Broussard, C. Tanaka, J. Nowak, J. Moodera, A. Barry, J. Coey, Science **282**, 85 (1998).
4 H. Kato, T. Okuda, Y. Okimoto, Y. Tomioka, K. Oikawa, T. Kamiyama, Y. Tokura, Phys. Rev. B **69**, 184412 (2004).

[5] M. Horne, P. Strange, W. Temmerman, Z. Szotek, A. Svane, H. Winter, J. Phys. Condens. Matter **16**, 5061 (2004).
[6] T. Shishidou, A. Freeman, R. Asahi, Phys. Rev. B **64**, 180401 (2001).
[7] I. Galanakis, P. Dederichs, N. Papanikolaou, Phys. Rev. B **66**, 174429 (2002).
[8] E. Şaşıoğlu, L. Sandratskii, and P. Bruno, Phys. Rev. B **72**, 184415, (2005).
[9] B. Balke, G. Fecher, J. Winterlik, and C. Felser, Appl. Phys. Lett. **90**, 152504 (2007).
[10] H. Kurt, K. Rode, M. Venkatesan, P. Stamenov, and J. Coey, Phys. Status Solidi B **248**, 2338 (2011).
[11] J. Winterlik, S. Chadov, A. Gupta, V. Alijani, T. Gasi, K. Filsinger, B. Balke, G. Fecher, C. Jenkins, F. Casper, J. Kübler, G. Liu, L. Gao, S. Parkin, and C. Felser, Adv. Mater. **24**, 6283 (2012).
[12] I. Galanakis, in *Heusler Alloys*, Springer Series in Materials Science 222, C. Felser and A. Hirohata (eds.), Springer International Publishing Switzerland 2016.
[13] P. Lukashev, P. Kharel, S. Gilbert, B. Staten, N. Hurley, R. Fuglsby, Y. Huh, S. Valloppilly, W. Zhang, K. Yang, R. Skomski, and D. Sellmyer, Appl. Phys. Lett. **108**, 141901 (2016).
[14] K. Hanssen, P. Mijnarends, Phys. Rev. B **34**, 5009 (1986).
[15] K. Hanssen, P. Mijnarends, L. Rabou, K. Buschow, Phys. Rev. B **42**, 1533 (1990).
[16] W. van Roy, M. Wojcik, E. Jdryka, S. Nadolski, D. Jalabert, B. Brijs, G. Borghs, J. De Boeck, Appl. Phys. Lett. **83**, 4214 (2003).
[17] S. Chaudhuri, D. Salas, V. Srihari, E. Welter, I. Karaman, P. Bhobe, Sci Rep **11**, 524 (2021).
[18] F. Mancoff, B. Clemens, E. Singley, D. Basov, Phys. Rev. B **60**(R12) 565 (1999).
[19] W. Zhu, B. Sinkovic, E. Vescovo, C. Tanaka, J.S. Moodera, Phys. Rev. B **64**, R060403 (2001).
[20] A. Caruso, C. Borca, D. Ristoiu, J. Nozieres, P. Dowben, Surf. Sci. **525**, L109 (2003).
[21] D. Ristoiu, J. Nozières, C. Borca, B. Borca, P. Dowben, Appl. Phys. Lett. **76**, 2349 (2000).
[22] I. Galanakis, J. Phys. Condens. Matter **14**, 6329 (2002).
[23] M. Ležaic, I. Galanakis, G. Bihlmayer, S. Blügel, J. Phys. Condens. Matter **17**, 3121 (2005).
[24] P. Kharel, W. Zhang, R. Skomski, S. Valloppilly, Y. Huh, R. Fuglsby, S. Gilbert, and D. Sellmyer, Phys. D: Appl. Phys. **48**, 245002 (2015).
[25] J. Herran, R. Dalal, P. Gray, P. Kharel, and P. Lukashev; J. Appl. Phys., **122**, 153904 (2017).
[26] F. Faid, M. Elchikh, S. Bahlouli, K. Kaddar, J. Supercond. Nov. Magn., **31**, 2491 (2018).
[27] V. Shukla, S. Kumar, J. Magn. Magn. Mater., **498**, 166111 (2020).
[28] V. Shukla, S. Kumar, J. Supercond. Nov. Magn., **33**, 3615 (2020).
[29] Y. Jin, J. Waybright, P. Kharel, I. Tutic, J. Herran, P. Lukashev, S. Valloppilly, and D. Sellmyer; AIP Advances **7**, 055812 (2017).
[30] A. Nelson, P. Kharel, Y. Huh, R. Fuglsby, J. Guenther, W. Zhang, B. Staten, P. Lukashev, S. Valloppilly, and D. Sellmyer; J. Appl. Phys., **117**, 153906 (2015).
[31] G. Kresse and D. Joubert, Phys. Rev. B **59**, 1758 (1999).
[32] P. Blöchl, Phys. Rev. B **50**, 17953 (1994).
[33] J. Perdew, K. Burke, and M. Ernzerhof, Phys. Rev. Lett. **77**, 3865 (1996).
[34] M. Methfessel and A. Paxton, Phys. Rev. B **40**, 3616 (1989).
[35] I. Galanakis, P. Dederichs, and N. Papanikolaou, Phys. Rev. B **66**, 134428 (2002).
[36] MedeA version 3.0; MedeA is a registered trademark of Materials Design, Inc., San Diego, USA.
[37] J. Towns, T. Cockerill, M. Dahan, I. Foster, K. Gaither, A. Grimshaw, V. Hazlewood, S. Lathrop, D. Lifka, G. D. Peterson, R. Roskies, J. R. Scott, N. Wilkins-Diehr, "XSEDE: Accelerating Scientific Discovery", Computing in Science & Engineering, vol.**16**, no. 5, pp. 62-74, Sept.-Oct. 2014.
[38] J. Rodríguez-Carvajal, Phys. B Condens. Matter. **192**, 55 (1993).
[39] I. Tutic, J. Herran, B. Staten, P. Gray, T. Paudel, A. Sokolov, E. Tsymbal, and P. Lukashev, J. Phys.: Condens. Matter **29**, 075801 (2017).
[40] T. Fichtner, G. Kreiner, S. Chadov, G. Fecher, W. Schnelle, A. Hoser, C. Felser, Intermetallics **57**, 101 (2015).
[41] Y. Jin, R. Skomski, P. Kharel, S. Valloppilly, D. Sellmyer, AIP Adv. **7**, 1 (2017).
[42] L. Longchar, M. Rahaman, B. Krishna Hazra, R. Rawat, M. Manivel Raja, S. Kaul, S. Srinath, J. Magn. Magn. Mater. **569**, 170439 (2023).